Final Draft
of the original manuscript:

Sign-inversion of charging-induced variation of electrical resistance of nanoporous platinum

Eva-Maria Steyskal and Maximilian Besenhard

Institute of Materials Physics, Graz University of Technology,

Petersgasse 16, A-8010 Graz, Austria

Stephan Landgraf

Institute of Physical and Theoretical Chemistry,

Graz University of Technology, Technikerstr. 4, A-8010 Graz, Austria

Yi Zhong

Institute of Materials Research, Materials Mechanics,

Helmholtz-Zentrum Geesthacht, Max-Planck-Straße 1, D-21502 Geesthacht, Germany

Jörg Weissmüller

Institute of Materials Physics and Technology, Eißendorfer Str. 42,

Hamburg-Harburg University of Technology, D-21073 Hamburg, Germany

Peter Pölt and Mihaela Albu

Institute of Electron Microscopy and Fine Structure Research,

Graz University of Technology, Steyrergasse 17, A-8010 Graz, Austria

Roland Würschum

Institute of Materials Physics, Graz University of Technology,

Petersgasse 16, A-8010 Graz, Austria[*]

(Dated: August 17, 2012)

1

Abstract

The electrical resistance (R) of nanoporous platinum prepared by dealloying reversibly changes by 4% upon electrochemical surface charging in a regime where oxygen adsorption/desorption and surface oxidation/reduction occurs. The variation of R with charging shows a sign inversion. Besides the usual behavior of increasing R with positive charging, a decrease of R occurs at higher potentials. Following recent studies of the sign inversion of the surface stress-charge response of porous nanophase Pt, the sign-inversion of the resistance with charging may be related to the electronic structure of the surface oxide. In addition, a charge-induced variation of the charge-carrier scattering rate at the metal−electrolyte interface is taken into account.

PACS numbers: 68.08.-p, 73.61.-r, 63.43.-h, 81.07.-b

* wuerschum@tugraz.at

2

I. INTRODUCTION

Highly porous nanoscaled metals open up a novel way of property tuning via the high number of surfaces. Upon immersing this kind of porous metals in an electrolyte, high surface densities of charge and adsorbates can be reversibly induced at the metal−electrolyte interface. In this way, voltage-induced reversible variations of the lattice spacing and macroscopic length [1] or, for instance, of the magnetic behavior [2, 3] of cluster-assembled porous nanocrystalline metals could be demonstrated. Even the properties of nanocrystalline oxides, e.g., the magnetic moment, can be modified via surface charging upon mixing the oxide nanoparticles with a porous conductive network of metallic nanoparticles for electrochemical charging [4].

Particularly attractive for surface charging are nanoporous metals prepared by dealloying such as nanoporous (np) Au [5] or np-Pt [6]. Compared to cluster-assembled nanocrystalline metals, effects associated with charging at surface-electrolyte interfaces emerge more pronounced in nanoporous metals prepared by dealloying owing to the reduced influence of interfaces between the crystallites, i.e., grain boundaries. Both charge-induced [7, 8] and surface-chemistry driven actuation (i.e., length change) [9] as well as tunable mechanical strength [10] could be observed in np-Au.

Electrical resistance in dependence of charging has been investigated so far for both particle-assembled porous nanocystalline metals (Pt [11], $Au_{75}Fe_{25}$ [12], [13]) as well as for nanoporous Au prepared by dealloying [14, 15]. In each of these studies the resistance was observed to increase reversibly upon positive charging, ranging from several percent up to 40 % when positive charging is extended to the regime of chemisorption [15]. The present work, reports on studies of the tunable electrical resistance of nanoporous Pt prepared by dealloying which shows a sign inversion from an increase to a decrease of the resistance with positive charging.

II. EXPERIMENTAL PROCEDURE

Nanoporous Pt was prepared by technique of electrochemical dealloying [5, 6, 16]. The master alloy $Cu_{75}Pt_{25}$ (at.%) was arc-melted from high purity Pt and Cu wires (Pt, 99.99%; Cu, 99.99+%) and subsequently homogenized at 1000 °C for 4 h. Thin foils were obtained

by rolling to a thickness of 120 μm. Between the rolling steps and afterwards the samples were annealed twice at 700 °C for 1 h. For dealloying stripes of ca. 18 mm×6 mm were cut. The samples were dealloyed at a constant potential of +1.15 V at ambient temperature (22±1 °C) in 1 M sulphuric acid under potentiostatic control versus a Ag/AgCl reference electrode using a tungsten rod (diameter 1 mm) as counter electrode. A salt bridge of 1 M KCl was used between the reference electrode and the electrolyte in order to avoid Cu precipation at the reference electrode. Dealloying was stopped when the current fell from an intial maximum value of ca. 9 mA/cm^2 to a value below ca. 0.1 mA/cm^2. After dealloying, the specimen was rinsed in distilled water and transfered from the dealloying cell into the measuring cell without intermediate drying. EDX analysis of np-Pt yields a residual Cu content of ca. $4-6$ at.% after dealloying.

The resistance measurements in dependence of electrochemical charging were performed in a similar way as decribed previously for measurements on np-Au [15]. Summarizing briefly, the nanoporous Pt stripe was contacted by five Pt wires, four electrodes for resistance measurement and one electrode for charging. The resistance was measured with the four-point method by means of a Keithley 2400 Source Meter. Charging was performed in an aqueous solution of 1 M KOH and controlled by a PGZ-100 potentiostat (Voltalab Comp.) with a counter electrode made of carbon cloth and with the potential being measured with respect to a commercial Ag/AgCl reference electrode filled with saturated KCl (Radiometer analytical). Contacting of the horizontally positioned, brittle sample was accomplished by vertically adjusting each of the Pt contact wires separately. For this purpose, each Pt wire was guided through a thin glass pipe onto the sample. The five contacts were arranged in line, using the central contact for charging, the two outermost for current supply, and the two in between for voltage measurement.

The resistance was monitored concurrently in intervals of 2.5 seconds during cyclo-voltametric (CV) scanning. Scans were performed at a rate of 1 mV/s unless stated else. The imposed charge was determined by integrating the charging current which was monitored continuously.

It was carefully checked that the electrochemical charging current did not affect the resistance measurements. On the one hand, upon reversing the direction of the R-measuring current by exchanging the outermost contacts, the same characteristics of R was observed. In addition, R values determined during CV were also confirmed by measuring R during

chronoamperometry (CA) at low residual currents which were at least one order of magnitude smaller than the charging current during CV.

III. RESULTS

Transmission electron microscopy after dealloying reveals a nanoporous structure with ligament diameters of $4 - 6$ nm and pore sizes in the range of several nanometers (Fig. 1). The porous structure is still present after heat-induced coarsening as shown in the scanning electron micrograph in Fig. 1.

Cyclic voltammograms after dealloying were taken between $+450$mV and -1100mV (measured versus Ag/AgCl) at a scan rate of 1 mV/s (see Fig. 2). This CV range is limited by oxygen- and hydrogen-evolution at the working electrode, respectively. As clearly visible in Fig. 2, the inital cycle after dealloying substantially differs from the subsequent ones which are typical for platinum according to textbook literature (e.g. [17]). The initial cycle, which starts scanning onwards from 0 mV, suggests that nanoporous Pt in as-dealloyed state is covered by strongly bound oxygen: Similarly as observed by Viswanath et al. [18] for surface-oxidized Pt at potentials above the oxygen desorption peak, the CV currents are low as the oxide remains in place. According to reference 18 the observed charge flow in this positive potential region of the initial cycle can mainly be attributed to capacitive processes (double layer charging), possibly accompanied by adsorption/desorption of weakly bound ions. During subsequent scanning in negative direction, a prominent peak with a maximum at ca. -850 mV occurs. Since this peak is only observed in the first cycle, it can be attributed to the desorption of the initial oxide layer formed during dealloying. The presence of a dealloying-induced, superficial oxygen state is also indicated by the charge accumulated during dealloying, which in each case was about 30 % larger than the value associated with dissolving copper completely from the master alloy.

Since the removal of the initial oxide layer caused damage of the platelet-shaped samples, the resistance measurements had to be limited to the potential regime between 0 mV to $+450$ mV in order to avoid oxygen desorption during charging. The variation of the resistance of nanoporous Pt (sample Pt-II) upon consecutive cycling in this voltage regime is shown in Fig. 3.a. A reversible resistance variation $\Delta R/R_0$ of about 4% occurs. Since scanning is limited to the narrow range of specific adsorption, this maximum variation $\Delta R/R_0$ is

5

much lower than that observed for nanoporous Au recently [15]. The most striking feature is that both during positive and negative scan, the resistance first increases and subsequently decreases, giving rise to relative resistance minima at the reversal points of the CV and to resistance maxima in between. This sign inversion of the direction of the resistance variation is more clearly visible in the $\Delta R/R_0 - U$ and $\Delta R/R_0 - Q$ plots shown in Fig. 3.b and c, respectively. For low potentials, denoted range A in the following, $\Delta R/R_0$ increases with increasing U, whereas for high potentials, denoted range B, the trend is inverted and $\Delta R/R_0$ decreases with increasing U. The potential at which the sign inversion occurs slightly differs from sample to sample, indicating that it sensitively depends on the oxygen adsorption or oxidation during the dealloying process. Moreover, the variation of R is also slightly dependent on the direction of scanning. Upon negative scanning, the transition between the regions A and B occurs at lower potentials and also the total variation of R is reduced, as shown by the reduced maxima.

With increasing number of cycles, the $\Delta R/R_0 - Q$ plots are progessively shifted towards higher Q-values (Fig. 3.c). This indicates an irreversible charge flow which presumably arises from the evolution of molecular oxygen at the electrode and from further oxidation of the sample upon positive scanning. In addition, the resistance slightly increases from cycle to cycle as indicated by the slight upward shift of the $\Delta R/R_0 - U$ curves (Fig. 3.b).

In order to study the sign inversion of the resistance variation in more detail, another nanoporous sample (Pt-I) was cycled separately within the ranges from 0 mV to +100 mV and from +350 mV to +450 mV which represent the regions A and B, respectively (see Fig. 4). Switching between regions A and B gives rise to a resistance variation of about 4% (see Fig. 4). Within the low potential regime A (Fig. 5.a), R reversibly increases (decreases) with increasing (decreasing) potential within a range of ca. 0.8%. As shown in the $\Delta R/R_0 - U$ plot (Fig. 5.b), only a slight hysteresis occurs between up- and downward scan in the low potential region. In the high potential region B (Fig. 6), the magnitude of the relative resistance variation is similar but the direction is inverted as already observed for the first sample (Pt-II, Fig. 3). As more clearly visible in the narrow scan regime applied for sample I (Fig. 6) compared to the wide scan regime of sample II (Fig. 3), the extrema of the resistance in the high potential regime are not in phase with U, but are lagging behind. This also becomes clear from the $\Delta R/R_0 - U$ plot (Fig. 6.b), showing that the resistance attains extrema in between the potential range.

6

This delayed response of R in region B compared to region A may indicate that the higher potential regime is governed by a slower process. Indeed, different time characteristics in the low and high potential regime may also be concluded from the fact mentioned above that the maxima in R observed for sample II depend on the scan direction (Fig. 3). Upon scanning downwards from the high potential regime, which is governed by the slower process, the maximum R-value is smaller than the second maximum reached during the upward scan from the low potential regime, where faster processes are assumed to prevail (see Discussion).

The sluggish response of R in region B is also demonstrated by measurements with different scan rates (sample Pt-III, Fig. 7). While for scanning with 0.5 mV/s the resistance variation is nearly in phase with the applied potential, with increasing scan rate the variation of R is increasingly lagging behind the applied potential. Moreover, the amplitude of the variation of R strongly decreases with increasing the scan rate, by a factor of 4 between the lowest and highest scan rate. From the damping of the amplitude with increasing scan rate a characteristic time constant of the slow process of approximately 50 s can be estimated. For the low potential region A, on the other side, no such dependence on scan rate is observed (not shown).

The details of the voltage-induced variation of R, particularly the sign inversion occurring between the low and high potential regime, are obviously dependent on the pre-history and the oxygen-related processes at high potentials. To gain further insight into the underlying processes, resistance measurements were performed after aging (sample Pt-IV, Fig. 8). In the initial state of this sample, a voltage-induced variation of R similar to those of the previous ones is observed, although the maxima upon negative scan are less pronounced and only visible as hump on the left side of the main maximum (compare the descending low voltage regime of sample IV, upper curve in Fig. 8, and of sample II, Fig. 3). After aging caused by prolonged cycling between 0 mV and +450 mV, this hump completely disappears (middle curve, Fig. 8). Obviously, in this aged state, the variation of R in the entire scan range (0 mV $-$ 450 mV) resembles that of the high potential region B of the previous samples, namely an increase (decrease) of R with decreasing (increasing) potential. This clearly demonstrates that the behavior in region B is related to oxygen coverage induced by prolonged aging at high potentials . This becomes even more evident by the fact that the initial $\Delta R/R_0 - U$ behavior can be recovered (bottom curve, Fig. 8) by partially removing the oxygen (without damaging the sample) upon keeping the sample at a low negative voltage of -50 mV for

several hours (bottom curve, Fig. 8).

IV. DISCUSSION

The most remarkable feature of the present studies is the reversible sign inversion of the charging-induced resistance variation. The resistance increases with positive charging in the regime of low potentials (regime A), whereas R decreases with positive charging for higher potentials (regime B).

A decrease of R with positive electrochemical charging as observed for regime A is a typical behavior. This has been observed before both for porous nanophase metals (nanocrystalline Pt [11], $Au_{75}Fe_{25}$ [12, 13], nanoporous Au [14, 15]) as well as for thin films [19] including Pt [20]. For sample II (Pt-II, Fig. 3) a charge coefficient $(\Delta R/R_0)/\Delta Q$ of about $+0.4 \times 10^{-2}$g/As is derived from the resistance increase (ca. 1.6%) in region A upon positive charging with an accumulated charge of $\Delta Q \approx 4.1$As/g. This charge coefficient is quite similar to that observed for nanoporous Au recently in the regime of specific adsorption (0.6 or 0.9×10^{-2}g/As [15]). Similar as discussed before for np-Au [15], the resistance increase in the chemical regime may be considered to arise primarily from charge carrier scattering since atoms in the chemisorbed layer at the metal−electrolyte interface may act as additional scattering centers.

Turning to the sign inversion of the charging-induced resistance variation, it should be noted at first, that a sign inversion of another charging-induced property variation has been observed recently for nanoporous Au [8] and nanocrystalline Pt [18], namely a sign inversion of the surface stress-charge coefficient. Clean metal surfaces usually are characterized by a negative value of the surface stress-charge coefficient, i.e., the surface stress in the double layer regime of charging increases with negative charging (electron excess). Since concomitantly with increasing surface stress the relative volume decreases, negative charging of porous nanophase metals in the double layer regime causes volume contraction (positive strain-charge response) which is considered to arise from the increasing strength of in-plane bonds due to excess electronic charge [8, 18]. Compared to this usual behavior, for oxide-covered porous nanophase metals (np-Au [8], nc-Pt [18]) the opposite behavior, namely a volume expansion with negative charging was observed. For nanoporous Au this behavior was only observed for the oxide-covered surface of the freshly dealloyed sample, whereas for

nanocrystalline Pt switching from the double layer behavior (positive strain-charge response) to the oxide-layer behavior (negative strain-charge response) could be achieved reversibly by appropriate electrochemical surface treatment. The volume expansion with negative charging (electron excess) in the partially oxidized sample is attributed to the filling of anti-bonding states of the surface oxide which weakens the bonds between surface atoms [18]. It should be mentioned that this behavior of the oxide-covered surface is different from the adsorption behavior where both H^+ and OH^- adsorption leads to an expansion due to stress relief upon adsorption [18].

Whereas the above mentioned sign inversion of the stress-charge coefficient occurs upon switching between the clean surface and the anodic adsorption regime, the sign inversion of the resistance, observed in the present work, occurs entirely within the anodic regime of adsorption of oxygen species. As described in Sect. III, the measurements had to be limited to this regime, since removal of the oxygen layer caused damage of the sample.

As mentioned above, Viswanath et al. [18] attributed the sign-inverted stress-charge response of porous nanocrystalline Pt to the particular charging characteristic of the partially oxidized surface. Such a scenario could also explain the present sign inversion of the resistance taking into account that Pt-oxide exhibits either semiconducting behavior or else metallic behavior similar as graphite with a minimum of the density of states at the Fermi edge [21]. Indeed, the resistance of graphite shows a sign inversion, i.e., R decreases both with negative and positive electrochemical charging since the electronic density of states increases in both directions of charging [22, 23]. Similarly also for semiconducting PtO the density of states [21] is expected to increase in both directions of charging which could explain a sign inversion.

The observation that with increasing amount of oxygen species the resistance first increases and subsequently decreases also exhibits some analogy with recent measurements of the electrical resistance of epitaxial Cu films with varying oxygen coverage [24]. The resistance was found to increase, decrease, and increase again with increasing oxygen coverage from the gas phase. This was attributed to partial specular surface scattering of electrons for smooth clean surfaces and for the surface with a complete adsorbed monolayer, but diffuse scattering at partial coverage and after chemical oxidation. Since in the present case oxygen species are adsorbed from the liquid phase, this notion presumably cannot be simply adopted here, nevertheless it shows that smoothening of the surface in the wake of adsorption may

cause a resistance decrease which also may prevail in the present regime B. Hence, as another explanation, alternative to the surface oxide given in the previous paragraph, within this picture the resistance first increases in regime A due to increasing charge scattering at the metal−electrolyte interface and subsequently decreases in regime B when with increasing adsorption the metal−electrolyte interface gets smoother.

A redeposition of Cu as well as a charge-induced volume variation may be ruled out as origin of the decreasing resistance with positive charging. In fact, an electrolytic deposition of Cu on Pt may provide additional charge carriers and thus may cause a decrease of R [25]. However, upon positive charging − if the case at all − Cu in the nanoporous Pt-sample is expected to be dissolved in the electrolyte rather than dissolved Cu being redeposited.

Regarding the effect of volume change, the dilatomteric studies of Viswanath et al. [18] have shown that nanophase Pt with a partially oxidized surface layer contracts upon positive charging. Although this corresponds to the correct sign of resistance variation, namely a decrease of R upon contraction or positive loading, the expected contraction is much too low (ca. one order of magnitude) in order to account quantitatively for the observed R decrease. This notion follows from a quantitative consideration of the pressure coefficient $(\Delta R/R)/p$ performed in the same manner as done previously for porous cluster-assembled nanophase Pt [11].

Finally (i) the delayed response of R at elevated positive potentials , (ii) the variation with scan rate, as well as (iii) the difference between scanning in negative or positive direction will be addressed. Each of these findings indicates that the high potential regime B is governed by a slower process. At sufficiently high potentials, oxygen adsorption and, beyond that, oxide formation, involving a kinetically limiting place exchange step, could be observed at platinum surfaces [26]. A delayed response of the resistance in the oxygen regime was already found by Dickinson and Sutton [20] for thin Pt films charged in H_2SO_4. Upon sweeping from the maximum positive voltage in negative direction, the amount of adsorbed oxygen was observed to grow further within a certain voltage range before desorption sets in. This finding agrees well with the present observation that in region B the reversal point of the resistance is lagging behind that of the voltage (Fig. 6). In addition to this delayed response, the slow process in regime B also explains the variation with the scan rate (Fig. 7) and scan direction (Fig. 3). The decrease of ΔR with increasing scan rate in this regime is obvious (Fig. 7). As far as the scan direction is concerned, upon scanning from the low

potential regime A into the high potential regime B, a higher R value is obtained due to a sluggish onset of the slow process B, whereas in the opposite scan direction the slow process fades slowly extending to potentials which belong to region A in the upward scan. This notion of a slow process in regime B is also consistent with the observed aging behavior (Fig. 8) which indicates that this slow process is oxygen related.

V. SUMMARY AND CONCLUSIONS

Nanoporous platinum was produced by dealloying of $Cu_{75}Pt_{25}$ in sulphuric acid. The samples reveal pore sizes and ligament diameters of several nanometers and are covered by superficial oxygen which could not be removed without irreversible sample damage. In the potential range, limited by this constraint, the electrical resistance could reversibly be tuned by several percent, exhibiting a sign inversion in the charge coefficient $(\Delta R/R_0)/\Delta Q$. Both regimes of charge coefficient exhibit different response times: whereas in the positive signed regime, R instantaneously varies with potential, the negative sign behavior is rather sluggish. While a positive charge coefficient, as observed for nanoporous Pt at lower potentials, is known from previous studies on nanoporous as well as nanocrystalline materials, a decrease of R at higher potentials has not been reported so far. Yet, a comparable behavior was observed in investigations of the surface stress-charge response. The sign inversion observed in this work may be attributed to the electronic structure of platinum oxide. Another explanation might be a modification of the superficial oxygen coverage upon charging, causing variations in the charge carrier scattering. For comparison, studies on compacted nanocrystalline platinum powder, oxidized under conditions similar to dealloying, would be desirable. Additional insight might also be gained from studying samples dealloyed with oxygen-free electrolytes.

[1] J. Weissmüller, R. Viswanath, D. Kramer, P. Zimmer, R. Würschum, and H. Gleiter, Science **300**, 312 (2003).

[2] H. Drings, R. Viswanath, D. Kramer, C. Lemier, and J. Weissmüller, Appl. Phys. Lett. **88**, 253103 (2006).

[3] S. Gosh, C. Lemier, and J. Weissmüller, IEEE Trans. on Magnetics **42**, 3617 (2006).

[4] T. Traußnig, S. Topolovec, K. Nadeem, D. Szabó, H. Krenn, and R. Würschum, phys. stat. sol. RRL **5**, 150 (2011).

[5] J. Erlebacher, J. Aziz, A. Karma, N. Dimitrov, and K. Sieradzki, Nature **410**, 450 (2001).

[6] D. Pugh, A. Dursun, and S. Corcorana, Mater. Res. **18**, 216 (2003).

[7] D. Kramer, R. Viswanath, and J. Weissmüller, Nano Lett. **4**, 793 (2004).

[8] H. Jin, S. Parida, D. Kramer, and J. Weissmüller, Surf. Sci. **602**, 3588 (2008).

[9] J. Biener, A. Wittstock, L. Zepeda-Ruiz, M. Biener, V. Zielasek, D. Kramer, R. Viswanath, J. Weissmüller, M. Bäumer, and A. Hamza, Nature Mater. **8**, 47 (2009).

[10] H.-J. Jin and J. Weissmüller, Science **332**, 1179 (2011).

[11] M. Sagmeister, U. Brossmann, S. Landgraf, and R. Würschum, Phys. Rev. Lett. **96**, 156601 (2006).

[12] C. Bansal, S. Sarkar, A. Mishra, T. Abraham, C. Lemier, and H. Hahn, Scripta Mater. **56**, 705 (2007).

[13] A. Mishra, C. B. M. Ghafari, R. Kruk, and H. Hahn, Phys. Rev. B **81**, 155452 (2010).

[14] A. Mishra, C. Bansal, and H. Hahn, J. Appl. Phys. **103**, 094308 (2008).

[15] P. Wahl, T. Traußnig, S. Landgraf, H.-J. Jin, and J. Weissmüller, J. Appl. Phys. **108**, 073706 (2010).

[16] H. W. Pickering, Corrosion Sci. **23**, 1107 (1983).

[17] C.H.Hamann and W. Vielstich, *Elektrochemie* (Wiley VCH, Weinheim, 1998).

[18] R. N. Viswanath, D. Kramer, and J. Weissmüller, Electrochim. Act. **53**, 2759 (2008).

[19] R. Tucceri, Surface Science Reports **56**, 85 (2004).

[20] T. Dickinson and P. R. Sutton, Electrochim. Act. **19**, 427 (1974).

[21] J. Uddin, J. E. Peralta, and G. E. Scuseria, Phys. Rev. B **71**, 155112 (2005).

[22] B. Kastening, M. Hahn, and J. Kremeskötter, J. Electroanalyt. Chem. **374**, 159 (1994).

[23] M. Hahn, M. Baertschi, O. Barbieri, J.-C. Sauter, R. Kötz, and R. Gallay, Electrochem. and Solid State Lett. **7**, A33 (2004).

[24] J. S. Chawla, F. Zahid, H. Guo, and D. Gall, Appl. Phys. Lett. **97**, 132106 (2010).

[25] M. Fujihira and T. Kuwana, Electrochim. Act. **20**, 565 (1975).

[26] B. E. Conway, Surf. Sci. **49**, 331 (1995).

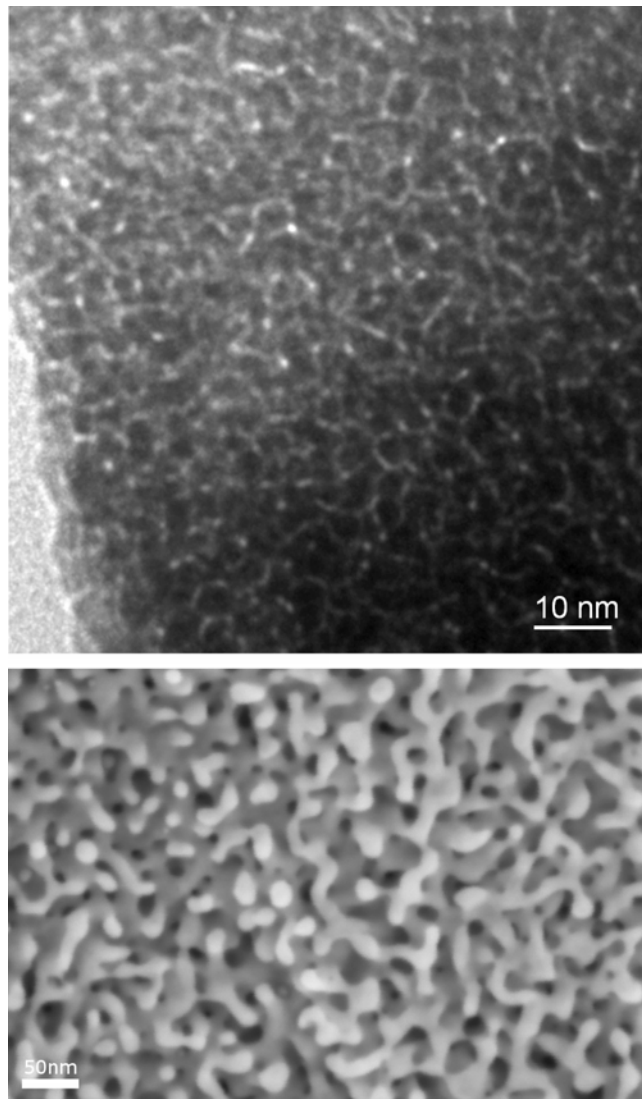FIG. 1. Electron microscopy of nanoporous Pt. Upper micrograph: transmission electron microscopy of as-dealloyed state showing pores in the range of 1 nm. Lower micrograph: scanning electron micrograph of nanoporous Pt after heat-induced coarsening.
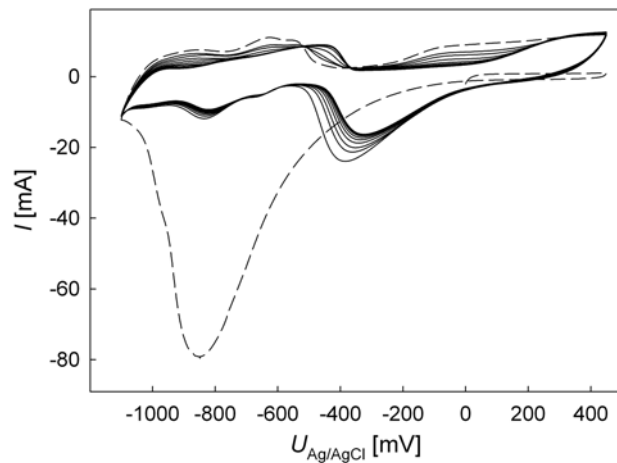
FIG. 2. Cyclic voltammograms of nanoporous Pt (sample Pt-I) scanned at 1 mV/s in 1M-KOH. I: current, U: voltage measured versus the Ag/AgCl reference electrode. The first cycle (dashed line) after dealloying significantly differs from the nine subsequent cycles (solid lines); measurement was started at 0 mV.
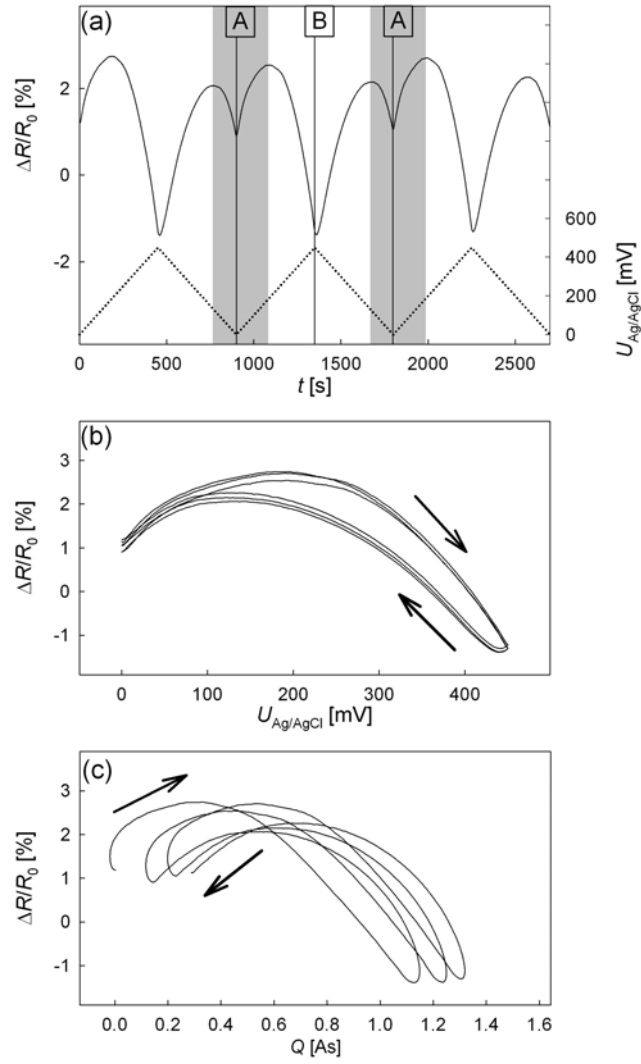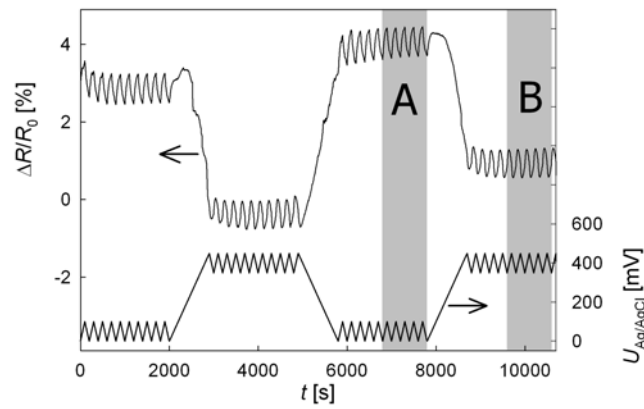
FIG. 3. Relative variation $\Delta R/R_0$ of resistance of nanoporous Pt (sample Pt-II) upon electrochemical cycling in 1M-KOH between 0 mV and 450 mV. (a) Variation of $\Delta R/R_0$ with time upon cycling of U with a scan rate of 1 mV/s. Low and high voltage regimes are denoted A and B, respectively. (b) Presentation of $\Delta R/R_0$ data in dependence of U. (c) $\Delta R/R_0$ in dependence of imposed charge Q. The reference value R_0 refers to the open circuit potential before charging procedures. U measured versus Ag/AgCl reference electrode.

16

FIG. 4. Variation of $\Delta R/R_0$ of resistance of nanoporous Pt (sample Pt-I) with time upon electrochemical cycling of U between 0 mV and +100 mV (region A) and between +350 mV and +450 mV (region B). Scan rate: 1 mV/s; electrolyte: 1M-KOH. U measured versus Ag/AgCl reference electrode.
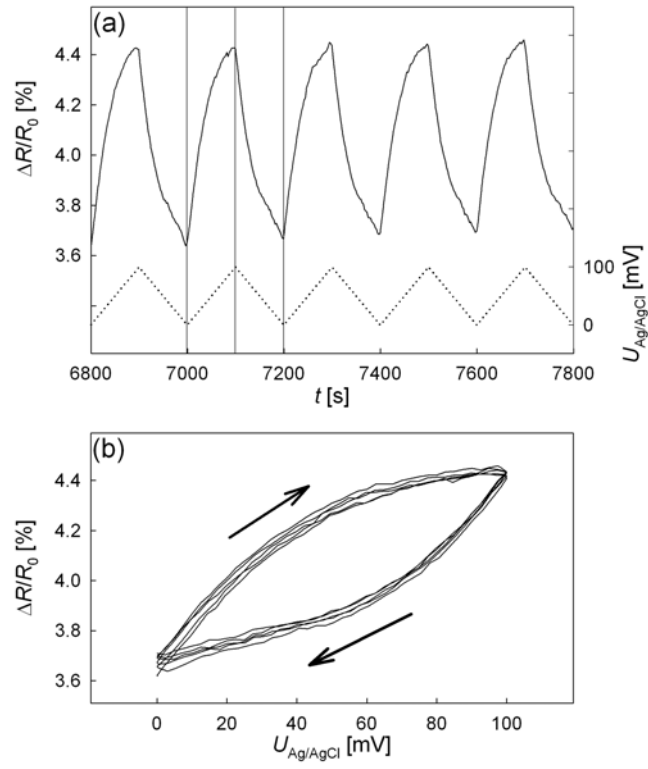
FIG. 5. (a) Region A zoomed from Fig. 4: Variation of $\Delta R/R_0$ with time upon cycling of U between 0 mV and +100 mV (for details see figure caption 4). (b) Presentation of $\Delta R/R_0$ data in dependence of U.
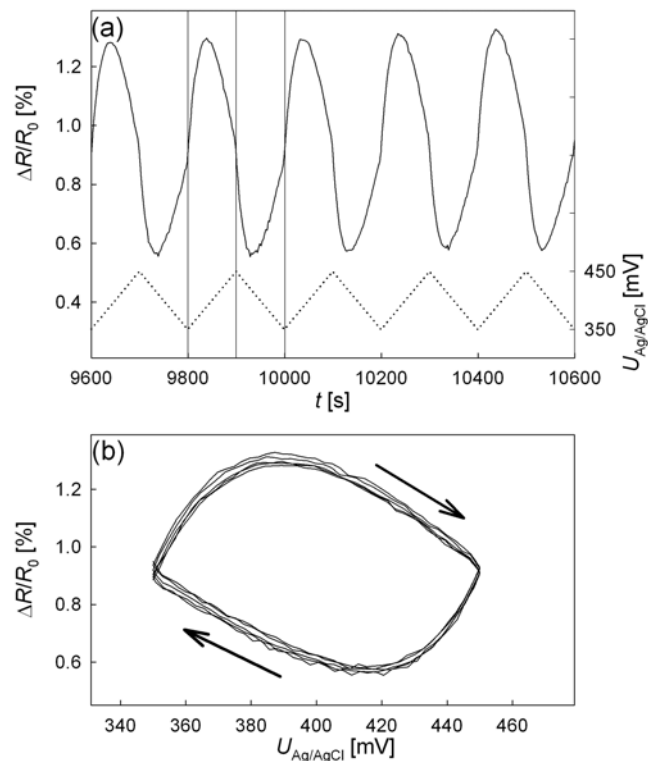
FIG. 6. (a) Region B zoomed from Fig. 4: Variation of $\Delta R/R_0$ with time upon cycling of U between +350 mV and +450 mV (for details see figure caption 4). (b) Presentation of $\Delta R/R_0$ data in dependence of U.
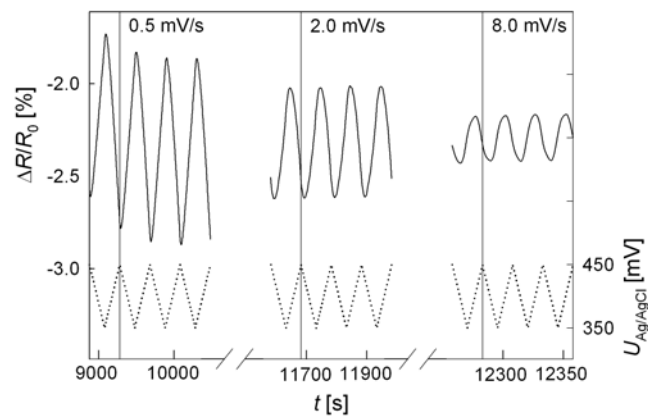

FIG. 7. Variation of $\Delta R/R_0$ upon scanning of U with different rates between +350 mV and +450 mV (corresponding to region B). Sample: Pt-III; electrolyte: 1M-KOH. U measured versus Ag/AgCl reference electrode.
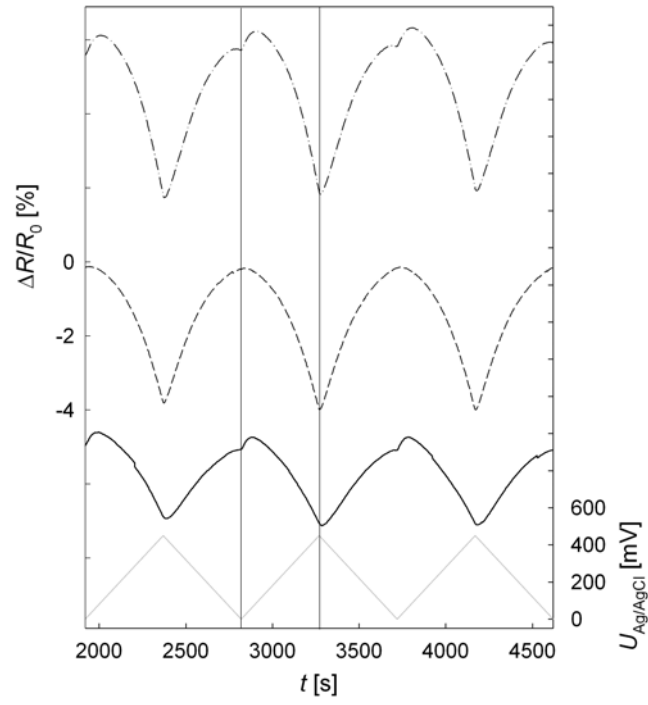
FIG. 8. Aging behavior of variation of $\Delta R/R_0$ upon cycling of U between 0 mV and +450 mV. Upper $\Delta R/R_0$-curve: initial state after dealloying; middle: aged state after multiple cycling between 0 and 450mV; bottom: regeneration of inital state after keeping at -50mV for several hours (solid). Sample: Pt-IV; scan rate: 1 mV/s; electrolyte: 1M-KOH. U measured versus Ag/AgCl reference electrode.